FINAL REPORT: NAG 3-741

MODELING OF SURFACE FLASHOVER ON SPACECRAFT

Contract NAG 3-741
1 September 1986 - 14 February 1990

Submitted by:

Mark J. Kushner
University of Illinois
Department of Electrical and Computer Engineering
1406 W. Green St., Urbana, IL 61801
(217) 244-5137 FAX (217) 244-7097

December 1991

I. Introduction

Although spacecraft usually have electrical systems that operate at voltages << 1 kV, there are proposals to launch spacecraft with pulse power modulators having operating voltages exceeding 100 kV.[1] These modulators will operate in a standby or ready mode until engaged. At that time the spacecraft will differentially charge (ie., different parts of the spacecraft will be charged to different potentials) and transients of many hundreds of kV may occur. Even in the absence of these modulators, spacecraft in geosynchronous orbit (GEO) and low earth orbit (LEO) interact with the local space environment resulting in the spacecraft charging to electrical potentials of many hundreds to a few thousand volts. The charging may be absolute, meaning that the spacecraft acquires a voltage with respect to the local space plasma potential, or the charging my be differential. When the differential electrical potential reaches some critical value, a surface flashover discharge (SFD) may occur. In an SFD, the electrical energy stored in the stray capacitance of the system is resistively dissapated through or on components of the spacecraft. In addition to physical degradation of materials, electronic systems may be damaged by voltage transients during an SFD. SFD's can occur on external surfaces of the spacecraft, or in internal cavities where an ambient atmosphere my be present due to outgassing of materials.

Although the self charging of spacecraft in GEO and LEO has been studied and is well understood,[2] the onset and methods to prevent SFD's are not well characterized. SFD's across solid insulators in vacuum have been investigated for many years due to the resultant loss of high voltage isolation and the damage which may occur.[2-7] A flashover discharge results from the random

emission of a relatively small number of electrons at the cathode which is the precursor to an electron avalanche towards the anode across the surface of the dielectric. A typical geometry, and that used in the study, is shown in Fig. 1. When using solid dielectrics for high voltage isolation, the source of seed electrons is usually electron emission from the cathode - vacuum - dielectric triple point.[8-11] Positive charging of the dielectric adjacent to the triple point by the seed electrons enhances the electric field there and helps sustain electron emission. As a result, the probability for the onset of flashover discharges, and the voltage at which they occur, often decrease as the thickness of the insulator decreases since the electric field enhancement, and hence electron emission, at the triple point increases. In applications where the surface or triple point are illuminated by UV radiation and the source of seed electrons is no longer dependent on the details of field emission from the triple point, the flashover voltage may not scale in the cited fashion. In fact, the flashover voltage may be lower by factors of 3-10 when the triple point or surface are illuminated by UV radiation than in the absence of irradiation.[12,13] The secondary emission and charging characteristics of the surface are equally as important in determining the flashover voltage as the initial emission mechanism for these conditions.[13] In most cases, though, the actual flashover voltage depends on a tradeoff between enhanced electron field emission and a lower probability for electron multiplication when the dielectric thickness is decreased.

An often quoted criterion for initiating a surface flashover discharge in vacuum over a plane dielectric is that the secondary emission coefficient,for the electrons striking the dielectric, δ, must be greater than unity.[7-14] For these conditions, electron multiplication occurs as the electrons scatter across the surface, charging the surface, and desorbing gas. Electron

multiplication, surface charging, and gas desorption are the precursors to other electron multiplication processes which perpetuate the discharge, such as gas phase ionization and further enhancement of the electric field at the triple point.[4,6,15] Most dielectrics possess this characteristic, $\delta \geq 1$, for some critical range of applied electric field. In complex geometries this simple criterion is difficult to apply since the orientation and value of the local electric field, and hence local secondary electron emission coefficient, are functions of position along the dielectric. In particular, the flashover voltage can depend on the angle of the dielectric with respect to the cathode and anode.[13] Another criterion is therefore required to characterize electron multiplication which accounts for the orientation of the electric field in a particular geometry, and for the past history of the surface.

In this research project a computer model has been developed to evaluate conditions leading to SFD's in complex geometries. The computer model is an electron Monte Carlo Simulation (EMCS) of electron scattering across dielectric surfaces while including charging of the dielectric, desorption of gas from the surface, electron-gas collisions, and ionization and excitation processes. The model is then used to investigate scaling relationships and methods which may be used to minimize the occurance of SFD's. The model will first be described in Section II, followed by a discussion of our parameteric results. In Section III, the use of surface transport coefficients in analyzing SFD's is discussed. In Section IV, the effects of geometry, surface roughness, gas additives and illumination of the triple junction are discussed in the context of minimizing the occurance of SFD's.

II. Description of the Model

A Monte Carlo particle simulation has been developed to model the scattering of electrons across the surface of a plane dielectric under high-voltage stress. The model uses as input the geometry and material properties of the electrodes and dielectric. In the simulation, we integrate the equations of motion of the electrons as they scatter from the dielectric while including secondary electron emission, backscatter, surface charging, and the deformation of the local electric field by surface charging. We can also include electron collisions with ambient or adsorbed gas resulting in scattering of the electrons, and excitation and ionization of the gas. Our emphasis is on conditions where the the rate of generation of seed electrons from the triple point is not a strong function of voltage, as may occur when the cathode or dielectric are illuminated by UV radiation.[12,13]

The geometry used in this work is shown in Fig. 1. The calculation is performed in three dimensions. The geometry shown in Fig. 1 is a two-dimensional "slice" through the dielectric and is perpendicular to the surface of the dielectric over which the electrons scatter. We use periodic boundary conditions in the plane of the dielectric, and so can use fairly narrow dimensions (mm's to a few cm) in that direction. Unless otherwise noted, quartz (δ_{max}= 2.4 at normal incidence) is used as the dielectric. During the calculation, a primary particle is given a pre-assigned "weighting", representing a given number of electrons (typically 10^5 electrons per particle), and is released from the triple junction at a single or distributed set of points along the line of intersection of the dielectric and cathode. The equations of motion of the particle are integrated, based on the local electric field (see below), and the trajectory of the particle is

updated. When a particle collides with the surface, the "weight" of the particle, w, is revised according to the backscatter yield, δ_b, for its energy and angle of incidence; $w \rightarrow \delta_b \times w$. If $\delta > 0$, then a particle is added to the simulation at the site of the collision to represent secondary electron emission. The weighting of the secondary particle is $(\delta - 1) \times w$. An electrical charge of $-qw \times (1 - \delta_b - \delta)$ is deposited on the dielectric surface at the site of the collision adding to the local charge density on the surface, $\rho(\mathbf{r})$. The secondary and backscatter yields as a function of energy and angle of incidence are used as tabulated in the NASA NASCAP program.[16] A plot of secondary emission coefficient as a function of angle of incidence and energy appears in Fig. 2. Since $\delta(\Theta) \sim \frac{1}{\cos \Theta}$, where Θ is measured from the normal, we in most cases restricted the value of δ to a maximum that corresponds to $\Theta = 80^0$ to account for microscopic surface roughness (see below).

A 3-dimensional electric field solver has been written using a combination of the method of Successive-Over-Relaxation (SOR)[17] and the superposition of fields from charges on the surface of the dielectric. This method considerably reduces CPU time and increases accuracy over that which is available from conventional "mesh" solutions. The method of SOR is first used to compute a 2-dimensional potential distribution one has in vacuum and in the absence of surface charging. SOR is an interative procedure which may be used to solve second order partial differential equations in the steady state. Using a five-point numerical molecule for couching finite differences, the updated potential at mesh point (i,j) on iteration k+1, ϕ_{ij}^{k+1} is given by

$$\phi_{ij}^{k+1} = (1-\alpha)\phi_{ij}^{k} + \alpha(a_{i-1,j}\phi_{i-1,j}^{k} + a_{i+1,j}\phi_{i+1,j}^{k} + a_{i,j-1}\phi_{i,j-1}^{k} + a_{i,j+1}\phi_{i,j+1}^{k}) \qquad (1)$$

where a_{ij} is a factor which accounts for differences in mesh size, boundary conditions and dielectric constants of the various materials. α is the SOR parameter which, under most conditions, $\alpha \simeq 1.7$. The SOR portion of the calculation is performed in 2-dimensions and the resulting potential distribution is differentiated to yield the electric field $E(r_2)$. (The subscript on r_2 denotes that this field is two dimensional.) If the boundary conditions (such as the electrode voltages or materials properties) change during the simulation, the fields can be updated.

The mesh used for the SOR calculation is adjustable in both directions. The need for this capability is dictated by the typical geometries of interest. For example, the "skimming" distance of an electron above the dielectric surface may be only 10s to 100s μm whereas the bulk electric field is determined by electrode structures have dimensions of many to 10s cm. In practice, the mesh used for the SOR is divided into a number of vertical regions, each having a constant mesh spacing. This is not a requirement of the SOR method, but evolved during program development. The SOR algorithm can be couched in a straight forward fashion to handle arbitrary meshes.

As the surface charge builds up as a result of secondary electron and ion emission, the local electric field "seen" by a charged particle includes contributions from both the applied bulk electric field and charges on the surface. In the simulation, the electric field at a given location $\mathbf{r}$ (three dimensional) and time is given by

$$E'(r,t) = E(r_2) - \sum_{i,j} (r - r_{ij}) \frac{\rho_{ij}(t)}{| r - r_{ij} |^3} \qquad (2)$$

where $\rho_{ij}(t)$ is the total charge at surface site (i,j) at time t. This surface charge is obtained by summing the net charge of all particles incident on that site including the effects of secondary emmision. This summation requires that the surface of the dielectric be discretized into a mesh. In practice, the summation is performed only in the vicinity of the electron and not over the entire surface. Since the electron can be very close to the dielectric it may "see" the charge predominantly only from a single computational cell on the horizontal surface. If that is the case, the charge associated with that cell is "smoothed" over its entire area to minimize steering effects which may occur as a result of charge being located at a single point.

The microscopic condition of the dielectric surface is quite important in determining the flashover voltage. It is well known that the secondary electron emission coefficient and the rate of desorption of gas from the surface are both functions of the angle of incidence of the electron. These quantities increase as the angle of incidence increases from normal to grazing. Electrons scattering across microscopically smooth surfaces therefore have the highest rate of secondary electron emission and of gas desorption because they can access grazing angles.

Any machined (or non-polished) surface is not microscopically smooth and, in fact, will have a "scratch and dig" of many to 10s of microns. In the simulation it would be computationally impractical to specify a particular surface morphology on these scales and explicitly calculate the local angle of incidence of an electron based on the local surface morphology. To account for surface roughness two algorithms were employed. In the first, we characterized the surface by a roughness factor, γ. In doing so, we restricted the angle of incidence of electrons to values $\leq (1-\gamma)\pi$ from the vertical. Atomically smooth surfaces have $\gamma = 0$ since electrons may arrive at grazing incidence. A

randomly rough surface having a morphology with vertical and horizontal excursions on the same scale will have a γ near unity.

In the second method used to model surface roughness, the surface represented is as being a sequence of isosceles triangles of specified relative heights (height/base). Larger relative heights correspond to rougher surfaces. When the electron strikes the surface, a random number [r = (0,1)] is chosen to determine the location of the strike relative to the base. This information, combined with the trajectory of the electron relative to a smooth surface produces a "roughened" angle of incidence.

Desorption of gas from the surface by electron impact is included in the calculation. The number of gas molecules desorbed per incident electron is not well characterized, but can be estimated in the fashion described below. Values from the literature indicate that 100-1000 gas atoms can be desorbed per incident electron. Once desorbed from the surface the position of the gas atoms is computed using a simple diffusion approximation

$$\frac{\partial N(\vec{r},t)}{\partial t} = Dv^2 N(\vec{r},t) \qquad (3)$$

where the "diffusion speed" is limited to a sonic value.

Gas desorption from the surface is believed to occur as a result of incident electrons ionizing adsorbed gas atoms. The resulting coulomb potential then accelerates the ion away from the surface. Neutralization simultaneously occurs on the outward trajectory.[18] The rate of electron impact stimulated desorption at location s on the surface, $\Gamma(s)$ (atoms/cm^2-s), can then therefore be approximated as

$$\Gamma(s) = \int_0^{\infty} \int_0^{\pi} \Phi_e(s,\epsilon,\Theta)\cdot\sigma_I(\epsilon)\cdot N(s)\cdot\left(\frac{1}{\cos\Theta}\right) 2\pi\cdot\sin(\Theta)d\Theta\, d\epsilon \qquad (4)$$

where $\Phi_e(x,\epsilon.\theta)$ $eV^{-1}st^{-1}$ is the incident electron flux at energy ϵ, $\sigma_I(\epsilon)$ is the ionization cross section of the adsorbed gas, N is the adsorbed gas density (cm^{-2}), and Θ is the angle of incidence measured from the vertical. The rate of desorption has a similar $(\cos \Theta)^{-1}$ dependence as secondary emission due to the effective increased path length through the near layers of the surface.

The Electron Monte Carlo Simulation (EMCS) is functionally similar to that described in Ref. 19 and so it will be only briefly described with emphasis on improvements to the previously reported model. A major improvement has been making the EMCS completely general with respect to gas composition. Based on the gas species which are specified to be included in the model, the required electron impact cross sections, anisotropic scattering factors and parameters for the distribution of secondary electrons produced during ionizations are extracted from a database. These parameters are entered into look-up tables for later use.

The electric field $E(\mathbf{r},t)$, obtained in the manner described above, for use in updating the trajectories of the particles is calculated for each "push" of the particles. The $E(\mathbf{r}_2)$ component of the electric field is interpolated from a two dimensional array during the calculation while the surface charge component of the field is updated in real time. The energies of the simulated electrons (typically 1000-5000) are initially randomly selected from a Maxwellian having a temperature of 1 eV.

The 2-dimensional electron energy distribution $f(\mathbf{r}_2,t)$ in the EMCS is formed by periodically recording the location and energy of each particle Numerically, f is an array known on a discrete volume of phase space $\Delta x_i \Delta y_j \Delta \epsilon_k$ centered on x_i, y_j, and ϵ_k. Collecting statistics involves determining the

(x_i, y_j, ϵ_k) bin which contains the phase space location of each electron and then incrementing $f(x_i, y_j, \epsilon_k)$ by an appropriate amount.

Ionization, attachment, and loss of electrons to the electrodes can change the number of pseudoparticles in the EMCS. When the number of pseudoparticles has increased or decreased by predetermined amounts, simulated electrons are removed or added (in a statistically unbiased fashion) to the EMCS. In the case of an increase in the number of particles, the mesh is divided into subregions and electron particles are removed in each subregion while insuring that the total charge is conserved. In the case of a decrease in the number of particles, more particles are released from the triple point. (The fact that particles are being preferentially removed from a given region in space is relevant information which must be retained.)

Electron collisions within the MCS are implemented using the efficient "null collision" algorithm.[20,21] Use of a modified version of the null collision algorithm allows electrons collisions with species whose densities evolve during the simulation to be easily included, such as desorbing gas or ions. Densities of ambient gas species are fixed and presumed known throughout the calculation. Densities of minor or evolving species (such as desorbing gas), however, are not initially known at the begining of the simulation. These leads to an ambiguity in selecting the electron collision frequency, a condition which is handled in the manner described below.

The electron kinetic energy range of interest is divided into a selected number of ranges. Each range k is divided into energy bins j centered on ϵ_{jk}. The width of the energy bins in each range is chosen to resolve any structure in the cross sections or structure expected in the electron energy distribution (EED). The total electron collision frequency in each energy interval υ_i (sequentially indexed from low to high electron energy) is

determined and probability arrays are initialized for each energy interval. The probability arrays are denoted P_{ij} for energy i and collision process j and are constructed such that

$$P_{ij} = \frac{\upsilon'_{ij}}{\upsilon_i}, \quad \upsilon'_{ij} = \sum_{\ell=1,j} \upsilon_{i\ell}, \tag{5}$$

where υ_{ij} is the collision frequency for energy interval i and process j, υ'_{ij} is the cumulative collision frequency for processes $\ell \leq j$, and P_{ij} is normalized so that for m processes, $P_{im} = 1$. A null or self scattering cross section is added to each energy interval so that the total (and maximum) collision frequency υ^{max}, including the null portion, is constant over a given energy range. (Here we suppress the index denoting the subrange.) The null collision process at energy ϵ_i has collision frequency $\upsilon^{null}(\epsilon_i) = \upsilon_i^{null} = \upsilon^{max} - \Sigma_j \upsilon_j(\epsilon_i)$, where the sum is over the collision process j. Using the Monte Carlo method, the time to the next collision is obtained from $\Delta t = -\ln(r_1)/\upsilon^{max}$, where r_1 is the first in a sequence of random numbers which are uniformly distributed on [0,1]. After updating the velocity and location of the particle using this time step, another random number is chosen. If $r_2 > \upsilon_i^{null}/\upsilon^{max}$, where the energy bin i is based on the instantaneous energy of the electron, then a real collision has occurred, and the particle velocity is revised accordingly. The specific collision which occurs is obtained by using r_2 to find the collision which satisfies

$$P_{i,j-1} < r_2 \leq P_{i,j}. \tag{6}$$

If $r_2 \leq \upsilon_i^{null}/\upsilon^{max}$, then a "null" collision occurs and the particle proceeds unhindered (that is, without changing its phase space coordinates) to its next

possible collision.

The energy resolved electron collision frequencies change during the simulation due to the changes in the density of charged and excited state densities. A modified null collision technique is used to avoid unnecessary recalculation of the collision probability arrays. The probability arrays described above are initialized using the electron impact cross sections for all ground state, excited species, ions and reaction products of interest. The densities of all of these species vary throughout the calculation and are not initially known. The collision frequencies are therefore calculated using the maximum expected density of each species i, n_i^{max}. n_i^{max} is known and fixed for the ambient gases, but n_i^{max} must be estimated for all species whose density evolves during the simulation. If during the simulation a collision with species i is selected at spatial location r, another random number r_3 is selected. If $r_3 \leq n_i(r)/n_i^{max}$, a real collision takes place and the collision algorithms are invoked. If $r_3 > n_i(r)/n_i^{max}$ then the collision is "null" and the particle proceeds unhindered.

III. Surface Townsend Coefficients

In gas discharges, transport coefficients are used to characterize various plasma processes as a function of E/N (electric field/gas number density).[22] One such coefficient is the Townsend coefficient, α (cm^{-1}), which is the characteristic distance for electron multiplication. α is defined by $n(z) = n(0) \times \exp(\alpha z)$, where $n(z)$ is the electron density at position z. Negative values of α denote net electron loss (e.g., recombination, attachment). It would be desireable to use similar coefficients for surface discharges to obtain scaling parameters so that the results from one experiment may be applied to other conditions, and so avoid the ambiguity of simply quoting δ.

In this section, we will use the results of our EMCS to show that electron transport across solid dielectrics, and the precursor conditions to initiating SFDs, can be characterized by a coefficient similar to the Townsend coefficient used in gas discharges. The coefficient represents the electron multiplication and charging characteristics of the dielectric material in the chosen geometry as a function of its charging history. The surface Townsend coefficient is defined by

$$\frac{\text{Number of electrons collected at the anode}}{\text{Number of electrons released at the cathode}} = \exp(\alpha \ell) \qquad (7)$$

where α is the Townsend coefficient of the insulator and ℓ is the length between cathode and anode. Two values of α are defined; α, based on the total emission; and α_i, the instantaneous value. A negative Townsend coefficient indicates a net loss of electrons as they scatter across the surface, and this instantaneously, denotes a non-flashover condition. A positive or zero

Townsend coefficient indicates no electron loss or net electron multiplication and is the precursor condition for a flashover. We will show that when the initial secondary electron emission does not depend upon field emission, $\alpha_i \geq 0$ is obtained at voltages significantly less than generally accepted as the flashover value.

A result of depositing charge on the dielectric by incident electrons having $\delta \neq 1$ is the formation of a sheath across the insulator surface. The sheath first forms near the cathode, where electrons initially strike the dielectric, and then spreads across the dielectric towards the anode. Immediately adjacent to the cathode, the surface charges positive. Away from the electrodes, the surface charge results in the sheath having a negative electric potential which is equal to the value which shields out the perpendicular component of the applied electric field within a few mm of the vacuum - dielectric interface. While the sheath is forming, the Townsend coefficient for electrons is negative since the source of charge on the dielectric is the emitted electrons. Following formation of the sheath at a particular location, electrons "pass" across the dielectric to a point of contact nearer to the anode in advance of the sheath, having on the average $\delta = 1$. By analogy, the formation of the sheath is equivalent to charging the capacitor formed by the cathode - dielectric - anode configuration. When the magnitude of released charge is sufficient for the sheath to cover the entire dielectric, the "capacitor" is fully charged. The magnitude of the local sheath potential at this time is such that the net secondary electron emission is unity. As a result, nearly the same number of electrons are collected at the anode as were emitted at the cathode, and the Townsend coefficient approaches zero.

Charging the dielectric and forming a sheath in this fashion are not

sufficient by themselves to initiate a flashover discharge since the end result of the charging is to drive the Townsend coefficient towards zero. Having $\alpha_i = 0$ corresponds to there being no net electron multiplication. However having $\alpha_i = 0$ with a fully charged sheath implies that the insulating properties of the surface have been compromised since a conducting path of near constant resistance exists between cathode and anode. It also emperically corresponds to the onset of a surface flashover.[13] If $\alpha_i = 0$ is approached from negative values one never does have net electron multiplication. If, however, a geometry and charge voltage results in an initially positive Townsend coefficient, then $\alpha_i = 0$ is approached from positive values. In this case, there has been an electron avalanche which results in the rapid desorption of gas from the surface. The desorption of gas is the precursor to secondary electron processes (e.g., gas phase ionization) which can further sustain electron avalanche and lead to flashover.[4,6,15] Therefore, the positive surface Townsend coefficient is a precursor to flashover, though it in itself is not a sufficient condition.

Electron multiplication or depletion is governed by the values of the secondary yield and backscatter yield parameters for the surface, which are functions of both electron energy and angle of incidence of the electron. In general, the electron backscatter and secondary yields increase as the angle of incidence approaches grazing.[23] Therefore, the orientation of the electric field with respect to the dielectric is important in determining the net rate of electron production. For our model geometry, the orientation of the electric field is a function of the thickness of the dielectric (see Fig. 3). The electric field is oriented more strongly into the surface with thin dielectrics, which results in low secondary emission, as well as low transverse mobility.

Typical electron energy distributions during the onset of an SFD are shown in Fig. 4. Average electron energies are only moderate, 10-25 eV. However there is a highly nonequilibrium tail to the electron energy distribution which extends to high energies (many 100s to 1000s eV). The low average energy results from a large influx of secondary electrons. The high energy tail of the distribution is fully capable of producing ionizing radiation when those electrons scatter off of the dielectric.

Surface Townsend coefficients for our model geometry calculated with the Monte Carlo particle simulation are plotted in Fig. 5 as a function of charge released from the triple point. The charge is released from the center of the cathode. We use the scaling parameter η = C-cm^{-1} (coulombs released / distance between the anode and cathode along the insulator surface). The values of α plotted in Fig. 5 are the integral values, α, corresponding to the total emission and collection of electrons. Therefore the condition $\frac{d\alpha}{d\eta} = 0$ corresponds to the instaneous value, α_i, being zero. In Fig. 5a, α is plotted for increasing anode-cathode voltage, V_o, having fixed length between anode and cathode, ℓ. We find that $\alpha_i = 0$ ($d\alpha/d\eta = 0$) is approached at an equilibrium charge that increases with increasing applied field. The initially negative values of α result from the dielectric in this geometry having, on the average, $\delta < 1$. As the surface charges and the sheath develops, α increases to reflect the fact that the average electron samples the surface less frequently, and the incident energy of the electron now corresponds more closely to that required for $\delta = 1$ due to the deceleration of the electron by the sheath. With higher applied fields, the average electron is more energetic as it approaches the surface, and therefore more charge is required to obtain this deceleration as shown.

In Fig. 5b, the cumulative α is plotted for fixed voltage with varying

length. The equilibrium charge scales well with the normalized charge η for these conditions. The amount of released charge required to reach equilibrium increases proportional to the length of the insulator for fixed voltage, as more charge is required to form the sheath over a larger area. Equivalently the capacitance of the configuration increases with length ($C = (\frac{\epsilon w}{d})\ \ell$, where w, ℓ and d are the width of the length, and thickness of the dielectric) and therefore more released electrons are required to charge the surface. The use of η is valid for linear scaling of a given geometry.

Our observation that $\alpha_i = 0$ is obtained at fixed η for constant charging voltage is consistent with the observation that flashover of UV illuminated surfaces occurs after a fixed incident fluence.[12,13] Our interpretation is that the fixed fluence corresponds to the photoemission of electrons sufficient to charge the dielectric to a condition where $\alpha_i \geq 0$ and shield out the perpendicular component of the applied field. There is, then, a nearly one-to-one correspondence between η and fluence. The observations of Enlo and Gilgenbach[12,13] that flashover occurs when the applied field is shielded by the sheath corresponding to $\alpha_i = 0$ confirms that this condition is a precursor to flashover.

As negative charge is deposited on the dielectric near the cathode, transverse components of the electric field are generated which may be comparable (> kV/cm) to the longitudinal field at the close approach (100's μm) of the scattered electrons to the charge. These space charge fields cause the electrons scattering across the dielectric to spread laterally, as shown in the plot of negative surface charge in Fig. 6. The negative charge continues to spread laterally until the sheath covers the surface. The areas devoid of negative charge adjacent to the electrodes are actually charge positive as has been predicted by other investigators.[4,6,7,23,24] The effect

of positive charge buildup at the cathode is to enhance the applied field, and consequently induce a greater number of particles per unit time to be released from the cathode. This induced emission from the triple point is also a precursor to flashover.

For our geometry, the electric field is oriented less strongly into the dielectric surface with thicker dielectrics. As a result, the average electron striking the surface does so with more energy and the secondary electron coefficients tend to be higher because of the advantagous scaling with grazing angle of incidence. The critical value of vacuum applied field for which the instantaneous and cumulative surface Townsend coefficients are positive, and $\alpha_i = 0$ is approached from positive values, therefore decreases with increasing dielectric thickness. The cumulative and instantaneous Townsend coefficents for such conditions are plotted in Fig. 7.

Accordingly, there is a trade-off between the magnitude of the applied electric field and the dielectric insulator thickness with respect to preventing a positive Townsend coefficient. This is shown by a parametric study of applied voltage and dielectric thicknesses (0 cm - 10 cm), summarized in Fig. 8. The parameter space can be divided into regions where α_i is always ≤ 0 (lower voltages for a given dielectric thickness) and where $\alpha_i > 0$ either instantaneously or cumulatively. Provided that electric field emission is not a necessary source of seed electrons as in a UV irradiated environment, thinner dielectrics are more likely to approach $\alpha_i = 0$ from negative values; thicker dielectrics are more likely to approach $\alpha_i = 0$ from positive values. The intermediate regime shown in Fig. 8 corresponds to there being high "shot to shot" variation in the charging. The end product of α_i approaching zero from either positive or negative values is there being no net electron multiplication. We propose, though, that the conditions where α_i approaches

zero from positive values is more prone to flashover due to the more intense positive field enhancement at the triple point and more rapid rate of gas desorption. We would then predict flashover voltages as low as 3-10 kv/cm for quartz under UV illumination, compared to 30-40 kv/cm for non-illuminated surfaces.[3,4]

Distortion of the local electric field by the sharp edges of the cathode and the discontinuity in dielectric constant at the triple point can produce local field enhancement of orders of magnitude. This may be sufficiently high to promote electric field emission of electrons. For our conditions, field enhancement and the probability for field emission increase as the thickness of the dielectric decreases. The electric field at the triple point, normalized by V_o/ℓ (where V_o is the vacuum applied voltage and ℓ is the anode - cathode separation) is plotted as a function of dielectric thickness in Fig. 9. As it is generally accepted that field emission occurs at field values of 500 kV-cm^{-1} - 1 MV-cm^{-1}, moderate values of V_o/ℓ with thin dielectrics may be sufficient to cause field emission.

As discussed above, thinner dielectrics in our geometry are less prone to rapidly obtaining $\alpha_i \geq 0$ and therefore by implication less susceptible to flashover discharges provided that field emission is the required source of seed electrons. However, thinner dielectrics maximize the probability for field emission. There is then, a tradeoff in dielectric thickness (or orientation of the electric field) with respect to flashover voltage when considering field emission and surface charging.

The insulating strength of the dielectric has been described in terms of an effective Townsend coefficient, α, and scaling parameter η (coulombs released/length of dielectric). The instaneous surface Townsend coefficient, α_i, approaches zero as η increases. A value of $\alpha_i \geq 0$ corresponds to

conditions which are the precursors to flashover discharges.[13] A trade-off exists between the flashover voltage and the thickness of the dielectric insulator. In the absence of field emission thicker dielectrics require a lower applied electric field to cause α_i to be ≥ 0. Thin dielectrics, though, are more prone to field emission at the triple point. With UV illumination, voltages resulting in $\alpha_i \geq 0$ (or $d\eta/d\alpha = 0$), are significantly lower than the flashover voltages measured in the absence of illumination. These results agree with experiments[12,13] and imply that obtaining high flashover voltages (exceeding many 10's of $kV\text{-}cm^{-1}$) depends on the suppression of the generation of seed electrons by illumination of the triple point or dielectric, or a reduction in the rate of charging of the dielectric.

IV. Methods to Minimize the Occurance of SFD's

A. Ambient and Injected Gases

The discussion in the previous section leads one to conclude that the most expedient strategy to prevent a SFD is to prevent charging of the surface. Once the surface is charged, then the net multiplication of the average electron in crossing from the cathode to the anode is zero; there may not necessarily be a catastrophic flashover event but the insulating properties of the dielectric have been compromised. To prevent surface charging one must insure that the net Townsend coefficient α remains negative and one must prevent enhancement of the electric field at the triple point. Charging of the surface and reduction in enhancement of the triple point can be accomplished by eliminating the source of seed electrons, "consuming" low energy secondary electrons (and seed electrons) as they are produced, and preventing gas phase ionizations. The use of high gas pressures works towards these latter goals. However, if $\exp(\alpha L) > 1$ in the gas phase or on the surface, then there is a statistical risk of a SFD occuring if seed electrons are allowed to propagate.

The active injection of gas onto the surface of the dielectric prior to charging is a mechanism whereby many of these goals can be met. First, electron collisions in the gas phase will reduce the electron energy and scatter electrons onto the surface in a more normal direction. This reduces the rate of electron secondary emission. There is, of course, risk that electron collisions in the gas phase will result in a net increase in ionization and hence defeat the original purpose. Many computer experiments were conducted using nonattaching gases (eg., He, N_2) to determine if there

was a parameter space in which low pressures of gas would reduce the onset of SFD's. No such parameter space was found. These results are consistent with the experimental results of Pillai and Hackam[25] who observed a similar increase in the flashover probability in air as compared to vacuum. The explanation is that gas phase ionization compensates for the reduction in mobility (and hence surface collision frequency) resulting from gas phase collisions. (See Fig. 10).

In injection of small amounts of attaching gases, though, were successful in preventing SFD's. As a demonstration system, we chose a F_2/NH_3 =1/1 mixture. This gas mixture is known to have a fairly large cross section for attachment for electron energies of < 10 eV. The probability for flashover for a 0.5 cm gap (10 kV charging voltage) is shown in Fig. 11 as a function of F_2/NF_3 presure. The SFD is quenched for a gas pressure > 10 Torr. (The electron avalanche is shown "stalling" in Fig. 10.) The gas pressure required to achieve this effect will increase with increasing voltage. The improvement is due to two effects. The first is the rapid attachment of low energy electrons which are emitted as a result of secondary processes which would otherwise participate in an avalanche process. The second is the fact that these electrons do not latter contribute to charging of the dielectric.

B. Passive Strategies

Although active flashover supression schemes such as that described above appear to work, one would ideally like a passive system since they are simplier and cheaper. One such method would be to alter the geometry of the dielectric to increase the tracking distance. Without implementing complicated structures, this passive mode appears less successful than the active mode

described above. We investigated the effect of ridges in the dielectric, as shown in Fig. 12. The time required for electrons to avalanche to 100 times their initial density time increased only marginally over the case for a flat dielectric. The reason for this behavior is that as the dielectric surface negatively charges and a sheath forms, the electrons are repelled and "hop" over the ridges. The details of this passive mode depend, of course, on the secondary emmission coefficient of the surface; this value has yet to be parameterized.

Another passive supression mode would be to have the gas that desorbs from the surface be a highly attaching gas. If the attaching gas is to have any effect on the surface avalanche process, the mean free path for attachment must be less that the mean free path (mfp) for electron multiplication. Assume that electron multiplication is due entirely to secondary electron emission from the surface with a mfp = λ_s. The mfp for electron attachment is $\lambda_a = (\sigma N)^{-1}$ where σ is the cross section for attachment and N is the density of the attaching gas. Furthermore, the thickness of the layer of attaching gas at the surface, l_s, must be at least a few attachment mean free paths so that the probability of collisions,

$$p = 1 - \exp(-l_s/\lambda_a) \approx 1. \qquad (8)$$

The attaching gas is evolved from the surface as a result of electron collisions at a rate proportional to the electron surface collision density, j_c. This rate is simply $R = nj_c$, where n is the number of gas atoms evolved per electron collision, and $j_c \approx \frac{j_e}{q} \cdot \min(1, \frac{\lambda_s}{l_e})$, where j_e is the electron current density above the surface, and l_e is the thickness of the electron swarm above the surface. Given this constant source function and diffusion

coefficient D, then the gas density at at position x above the surface at time t is

$$N(x,t) = \frac{j_c}{D}\left(\left(\frac{Dt}{\pi}\right)^{1/2}\exp(-x^2/(4Dt)) - \frac{x}{2}\,\mathrm{erfc}\left(\frac{x}{2(Dt)^{1/2}}\right)\right) \qquad (9)$$

The time at which desorption of an attaching species from the surface results in a depth and density of gas so that quenching of the flashover discharge will occurs is when

$$N(3\lambda_s,t) >> \frac{1}{\sigma\lambda_s}. \qquad (10)$$

Using typical values of n = 100, D = 150 cm^2/s-Torr, $\sigma = 10^{-16}$ cm^2, l_e = 0.25 cm, j_e = 10 A/cm^2, and λ_s = 0.1 cm, N exceeds the critical value at 10-50 μs, which is long compared to the kinetics time scales over which the avalanche may occur ($\approx$ 10 ns). Therefore, there appears to be a "window of vulnerability" in which desorbing gas may actually be a detriment to holdoff. If, however, enough of the gas can be desorbed to generate a critical area density, the attaching nature of the gas may quench the SFD in its formative stages. (See Fig. 13)

One aspect of the initiation of SFDs which is not directly addressed by the model is the increase in field emission at the triple point that may occur as a result of triple point enhancement. Triple point enhancement is an increase in the triple point electric field due to positive charge generated on the dielectric in front of the triple point. The larger the degree of triple point enhancement, the greater the probability that a SFD will occur. The use of low pressures of attaching gas can significantly decrease the rate

of charging of the dielectric in front of the triple point, and hence decrease the probability for onset of a SFD. Triple point enhancements depend on the voltage and geometry of the triple point. Typical triple point enhancements are shown in Fig. 14.

The effects of low pressures of attaching gas on the triple point enhancement are shown are shown in Fig. 14. Here we compare the triple point enhancment for the ambient being a vacuum and the 10 Torr F_2/NF_3 = 1/1 mixture. The triple point enhancement is decreased by a factor of two using the attaching gas.

C. Surface Roughness

Secondary electron emmission from surfaces caused by electron impact scales as $(\cos \Theta)^{-1}$, where Θ is the angle of incidence (as measured from the normal). On atomically smooth surfaces scattering electrons can access grazing incidence angles. The rate of secondary electron emission is very high, thereby leading to avalanche and the onset of an SFD. If a surface is microscopically rough (roughness lengths which are commesurate with the scattering distance) then the average angle of incidence of electrons scattering on the surface is decreased, and so the secondary electron yield is decreased. (An electron scattering on a surface having a "picket fence" morphology will experience many normal incidence collisions.). One may be able to capitalize on these trends by micromachining a surface to have a preselected degree of roughness, and therefore control, to some degree, the amount of secondary electron emission.

This method of control was investigated with the results shown in Fig. 15. The voltage at which an SFD will occur is plotted as a function of a

parameter indicating the relative roughness of the surface. The larger the roughness factor, the smaller the average angle of incident of electrons scattering on the surface. A roughness factor of 0 represents an atomically smooth surface; a roughness factor of 1 represents a "picket fence" morphology. There is a significant increase in the flashover voltage with the roughess factor exceeds 0.3, which corresonds to the angle of incident being largely confined to a cone of 65^{o} from the vertical, thereby eliminating the majority of grazing angle collisions.

Over longer time scales, microscopic surface roughness will not be a dominant factor in preventing SFDs. Once the surface negatively charges, scattering electrons will be shielded from any microscopic roughness, and on the average "move over" the roughness. The roughness can, however, have an important effect in the formative stages of an SFD, perhaps delaying electron avalanche for a sufficiently long period that any transient can be survived. An example of this effect is shown in Fig. 16 where the first Townsend coefficient for electron scattering is shown as a function of position between the cathode and anode. The Townsend coefficient for the rough surface is significantly smaller than the smooth surface, thereby delaying the onset of avalance. In the absence of magnetic fields (see below) Krompholz et. al.[26] In the absence of magnetic fields (see below) Krompholz et. al.[26] observed increases in the flashover voltage for rough G-10 surfaces compared to smooth surfaces.

C. Magnetic Insulation

Magnetic insulation is a method whereby the flashover voltage of surfaces may be increased by perturbing the trajectories of electrons scattering over

the surface. Electron impact desorption of gas from the surface is believed to be a precursor to SFDs. A magnetic field which is both perpendicular to the surface and to the applied electric field will reduce the rate of desorption. Analogously, electrons can be "lifted" off the surface by a magnetic field parallel to the surface and perpendicular to the electric field so that E x B drift is out of the surface. Similar arguements can be made with respect to secondary electron emission. Since secondary electron emission depends upon the angle of incidence, an externally applied magnetic field can either increase or decrease the rate of secondary electron emission, depending on the average perturbation of the angle of incidence.

We investigated the onset of SFDs in the presence of an externally applied magnetic field. The orientation of the field was parallel to the surface of the dielectric and perpendicular to the applied electric field. The results are shown in Fig. 17. Applied B-fields of < 0.1 Tesla actually increased the rate of secondary electron emission, and hence reduced the voltage at which the SFD began. Sufficiently large B-fields, resulted in a decrease in secondary electron emission and, eventually, reached the lift-off condition where the electrons are magnetically insulated from the surface. This increases the voltage at the onset of an SFD. These results are in general agreement with the experiments of Krompholz et al.[26]

E. Consequences of UV Illumination

Enloe and Gilgenbach performed a series of experiments during which the flashover voltage of insulators was measured in the presence of UV illumination of either the dielectric, triple point or both.[12,13] The source of the UV radiation was a KrF laser (248 nm). The UV illumination serves to

charge the surface by secondary electron emission, and desorbs gas to some degree. In general, Enloe and Gilgenbach observed that the flashover voltage decreased with increasing UV illumination. Flashover was effected when a critical UV fluence was applied, implying that some critical amount of surface charging was required. The amount of surface charging is that value which generates electric fields which are commensurate with the applied electric fields. Flashover occured on either the rising or trailing edge of the UV illumination pulse, depending on when the critical fluence was delivered.

We investigated this phenomenon in the context that the UV illumination charges the surface of the dielectric, and our results are shown in Fig. 18. Low values of voltages, which do not cause an SFD in the the absence of UV illumination will develop into a SFD with UV illumination. We found that larger UV fluences are required at lower voltages, in agreement with the experiments. The onset of SFDs appeared to be more sensitive to UV fluence when only the dielectric was exposed to UV illumination compared to also illuminating the triple point.

V. Concluding Remarks

A model for predicting the onset of surface flashover discharges in the context of high voltage pulse power modulators has been developed and used to investigate mechanisms leading to the onset of SFDs, as well as strategies to minimize that onset. We have demonstrated that it is possible to analyze surface discharges in a manner similar to gas phase discharges using transport coefficients such as the first Townsend coefficient. Our parameterization of various methods to prevent, or at least delay, the onset of SFDs was not particularly successful in that many of the strategies which we investigated do not yield significantly improved performance. Established techniques may be applied which use, for example, magnetic insulation. The pulse power apparatus which would be required to supply these magnetic fields would itself be large and heavy, thereby possibly precluding its use on spacecraft. Any geometrical strategy (e.g, surface roughess, grooves, ridges) may be temporarily effective, but will ultimately be compromised by surface charging. The only safe strategy to reduce the occurance of SFDs is to prevent the dielectric from being charged in the first place. This leads one to consider passive or active schemes which employ low pressure of attaching gases which flood the surface prior or coincident to pulsing the high voltage apparatus. Our calculations indicate that only moderate amounts of gas (10s Torr effective pressure at the substrate) would be sufficent for many of the anticipated applications. If the surface is flooded only when high voltage is applied across the dielectric, the gas consumption would be nominal.

References

1. G. Yonas, "Importance of Pulsed Power to the Strategic Defense Initiative", 5th IEEE Pulsed Power Conference, Arlington, VA, 1985.
2. C. K. Purvis, H. B. Garret, A. C. Wittlesey and N. J. Stevens, "Design Guidelines for Assessing and Controlling Spacecraft Charging Effects", NASA Tech. Paper 2361, Sept. 1984.
3. Eoin W. Gray, J. Appl. Phys. **53**, 237 (1982).
4. Eoin W. Gray, J. Appl. Phys. **58**, 132 (1985).
5. A. A. Avdienko, Sov. Phys. Tech. Phys. **22**, 982 (1977).
6. A. Sivathanu Pillai and Reuben Hackam, J. Appl. Phys. **53**, 2983 (1982).
7. T. S. Sudarshan, J. D. Cross and K.D. Srivastava, IEEE Trans. Electr. Insul. **EI-12**, 200 (1977).
8. A. Sivathanu Pillai, R. Hackam and P. H. Alexander, IEEE Trans. Electr. Insul. **EI-18**, 11 (1983).
9. M. J. Kofoid, AIEE Trans. (Power App. Syst.) **79**, 999 (1960).
10. T. S. Sudarshan and J. D. Crow, IEEE Trans. Electr. Insul. **EI-8**, 122 (1973).
11. J. E. Thompson and M. Kristiansen, IEEE Trans. Plasma Sci. **PS-8**, 191 (1980).
12. C. L. Enloe and R. M. Gilgenbach, Plasma Chem. Plas. Proc. **7**, 89 (1987).
13. C. L. Enloe and R. M. Gilgenbach, Trans. Plasma. **PS-17**, 550 (1989)
14. T. S. Sudarshan and J. D. Cross, IEEE Trans. Electr. Insul. **EI-11**, 32 (1976).
15. A. A. Avdienko and M. D. Malev, Sov. Phys. Tech. Phys. **22**, 986 (1977).
16. C. K. Purvis, "Effects of Secondary Yield Parameter Variation on Predicted Equilibrium Potential of an Object in a Charging Environment," NASA Technical Memorandum 79299, 1979.
17. W. F. Ames, "Numerical Methods for Partial Differential Equations" (Academic, New York, 1977), Ch. 3.
18. J. H. Leck and B. P. Stimson, J. Vac. Sci. Tech. **9**, 293 (1971)
19. M. J. Kushner, J. Appl. Phys. **61**, 2784 (1987)
20. H. R. Skullerud, J. Phys. D **1** 1567 (1968).
21. S. L. Lin and J. N. Bardsley, J. Chem. Phys. **66** 435 (1977).
22. B. Chapman, *Glow Discharge Processes* (John Wiley & Sons, 1980), pp. 77-132.
23. J. I. Goldstein, D. E. Newbury, P. Echlin, D. C. Joy, C. Fiori and E. Lifshin, *Scanning Electron Microscopy and X-Ray Microanalysis* (Plenum Press, New York, 1981), pp. 53-95.
24. C. H. de Tourreil and K. D. Srivastava, IEEE Trans. Electr. Insul. **EI-8**, 17 (1973).
25. A. S. Pillai and R. Hackam, J. Appl. Phys. **58**, 146 (1985)
26. H. Krompholz, R. Korzekwa, M. Lehr and M. Kristiansen, SPIE Vol. 871 page 341 (1988)

Figure Captions

1. Geometry used in this study. The cathode and anode are separated by a planar quartz dielectric surface. Electrons are emitted from the cathode triple point.

2. Secondary emission coefficient for electrous scattering from quartz as computed from Ref. 16

3. Typical electrical postential prior to an SFD. There is no charge on the dielectric. For this geometry the electric field is oriented more strongly into the dielectric as the thickness of the dielectric decreases.

4. Typical electron energy distribution at the onset of an SFD. The large number of low energy electrons result from secondary electron emission.

5. Cumulative Surface Townsend coefficient as a function of η (charge released from the triple point/distance between cathode and anode) for the geometry shown in Fig. 1 using a quartz dielectric of 3.5 mm thickness. The coefficients are for the integrated released and collected current. a) Townsend coefficients for different cathode - anode voltage with fixed separation. b) Townsend coefficients for fixed voltage and different cathode - anode separation.

6. Location of negative charge as a function of released charged from the triple point for conditions where $\alpha < 0$. The view is looking down on the dielectric with the cathode at left and anode at right. The apparently uncharged regions adjacent to the cathode and anode in c) actually have positive surface charge.

7. Instantaneous and cumulative surface Townsend coefficients where $\alpha \geq 0$. The dielectric thickness is 1.5 cm. The Townsend coefficient builds from a negative value to a positive value as the released charge initiates an avalanche that eventually extends all the way to the anode. Obtaining a positive Townsend coefficient is a precursor to flashover.

8. Regions of negative and positive surface Townsend coefficient in the voltage - dielectric thickness plane for the geometry shown in Fig. 1. There is a trade-off between the magnitude of applied electric field and the thickness of the dielectric with respect to insuring that $\alpha_i \leq 0$. The intermediate region corresponds to having high shot to shot variation.

9. Electric field at the triple point (normalized by $E_o = V_o/\ell$ where V_o is the vacuum applied voltage and ℓ is the anode - cathode separation) as a function of dielectric thickness for the geometry shown in Fig. 1. For our conditions, field enhancement and the probability for field emission, increase as the thicknesss of the dielectric decreases.

10. Electron swarms as a function of position for (top) vacuum, (middle)

500 Torr of ambient He, and (bottom) 10 Torr of ambient F_2. Small amounts of an attaching gas such as F_2 are able to quench the SFD by "consuming" the low energy secondary electrons which are produced.

11. Probability for initiating a SFD as a function of ambient pressure of a F_2/NF_3 = 1/1 mixture. Only small amounts of attaching gas are required to prevent charging of the insulator.

12. Electron swarms for a dielectric with macroscopic ridges. The ridges are not effective in preventing the electron avalanche because a sheath forms at the surface which allows the electrons to "pass over" the macroscopic features.

13. Neutral gas density desorbing from the dielectric after 2.5 μs of electron scattering with an average current density of 10 A-cm^{-2}.

14. Enhancement in the electric field at the triple point with and without an ambient attaching gas (10 Torr F_2/NF_3). Reduction in the charging of the insulator in front of the triple point by the attaching gas reduces the triple point enhancment.

15. Flashover voltage as a function of microscopic roughness of the surface. As the roughness increases, the average angle of incidence also increases, thereby decreasing secondary electron yields.

16. First Townsend coefficient as a function of position between the cathode and anode. Two cases are shown; microscopically smooth and microscpically rough surfaces. The rougher surface is more "attaching", and therefore reduces the propensity for avalanche.

17. Flashover voltage as a function of applied magnetic field. The initial decrease in flashover voltage results from an increase in the grazing angle of incidence of electrons. The increase at larger applied fields is partly due to the "lift-off" phenomenon.

18. Probability for flashover as a function of the UV illumination of the substrate. With increasing illumination, there is more surface charging, thereby decreasing the voltage at which flashover will occur.

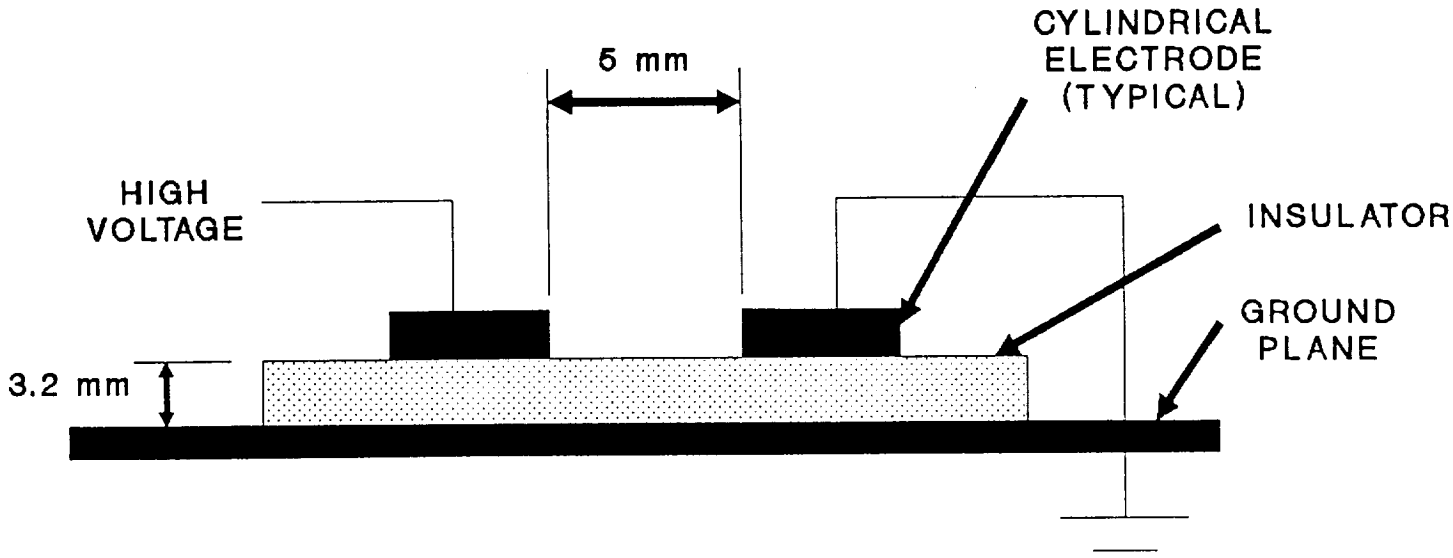

Figure 1

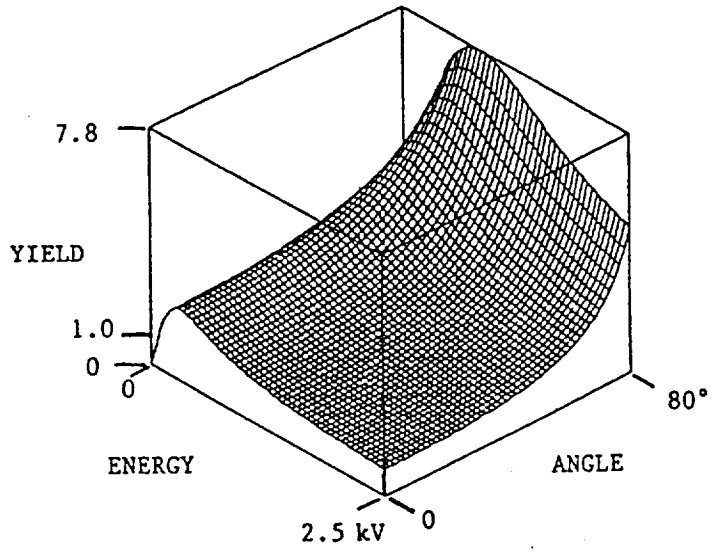

Secondary Yield (Quartz)

Figure 2

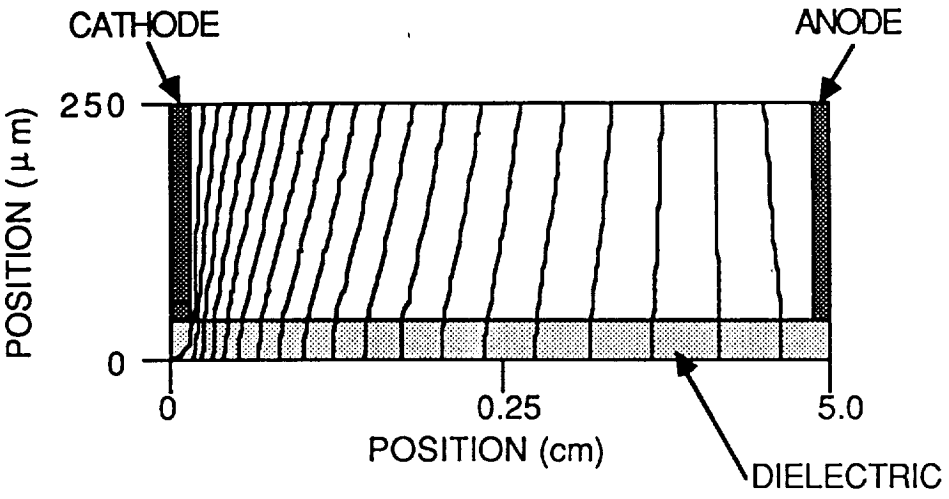

Figure 3

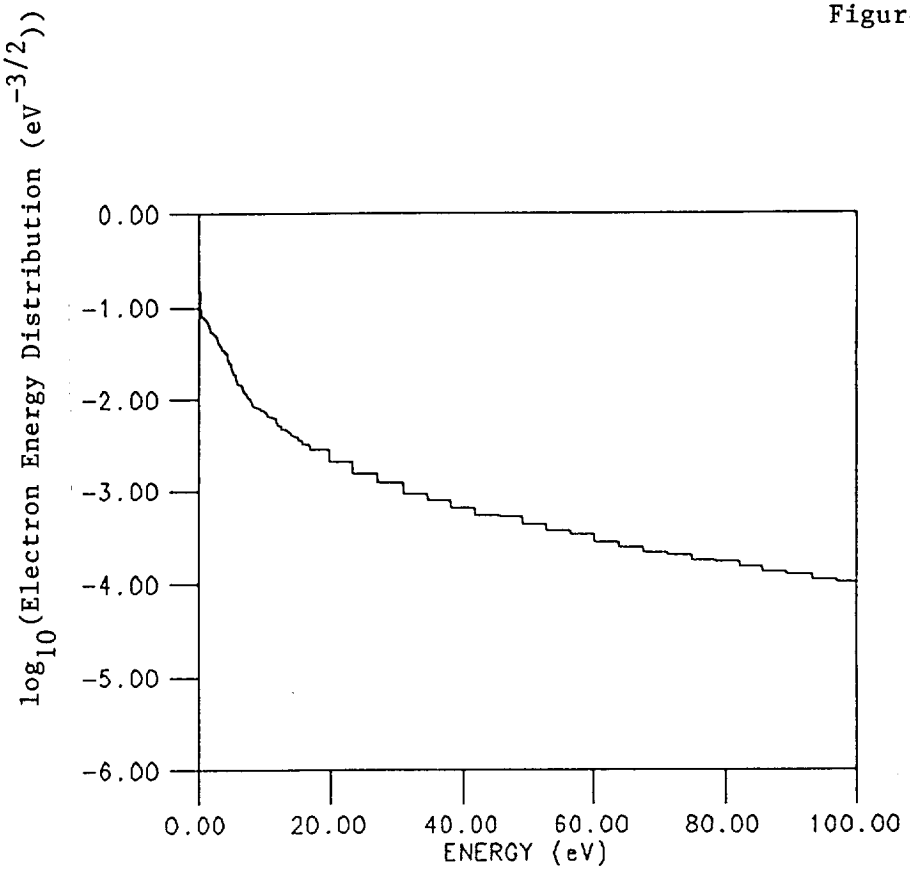

Figure 4

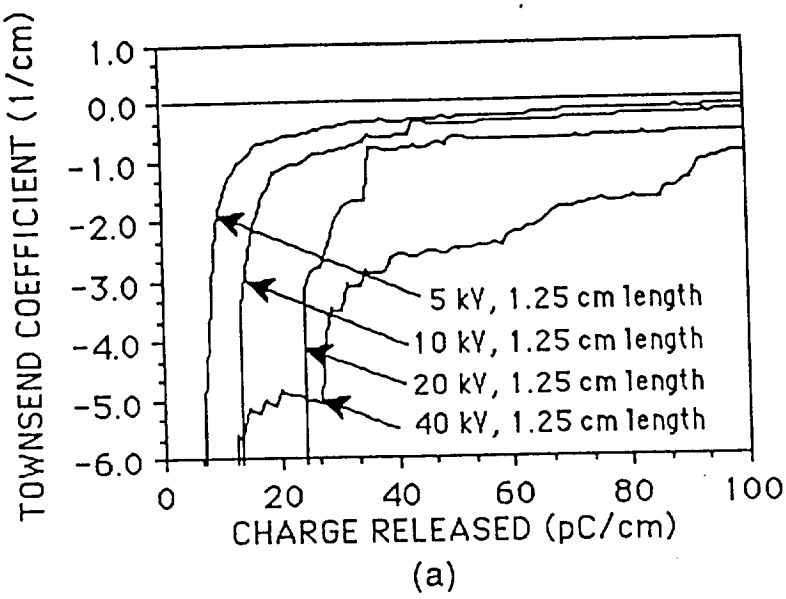
TOWNSEND COEFFICIENT (1/cm)
1.0
0.0
-1.0
-2.0
-3.0
-4.0
-5.0
-6.0
0
20
40
60
80
100
CHARGE RELEASED (pC/cm)
5 kV, 1.25 cm length
10 kV, 1.25 cm length
20 kV, 1.25 cm length
40 kV, 1.25 cm length
(a)

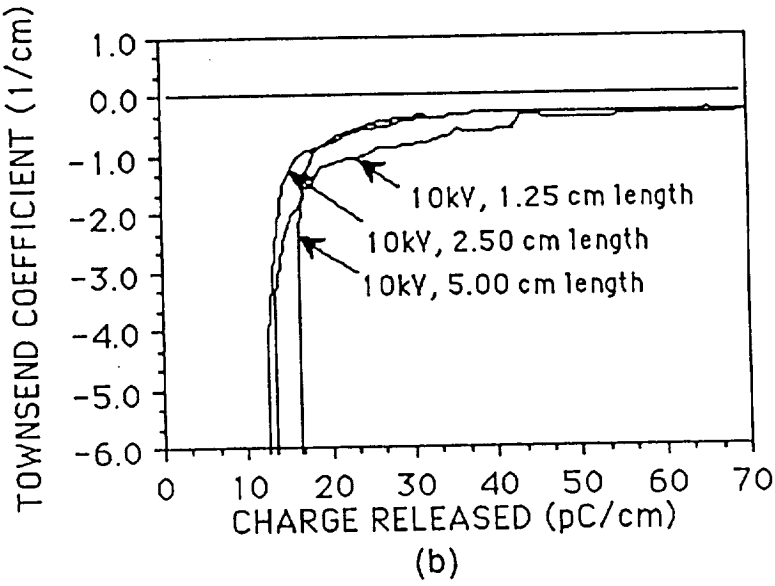
TOWNSEND COEFFICIENT (1/cm)
1.0
0.0
-1.0
-2.0
-3.0
-4.0
-5.0
-6.0
0
10
20
30
40
50
60
70
CHARGE RELEASED (pC/cm)
10kV, 1.25 cm length
10kV, 2.50 cm length
10kV, 5.00 cm length
(b)

Figure 5

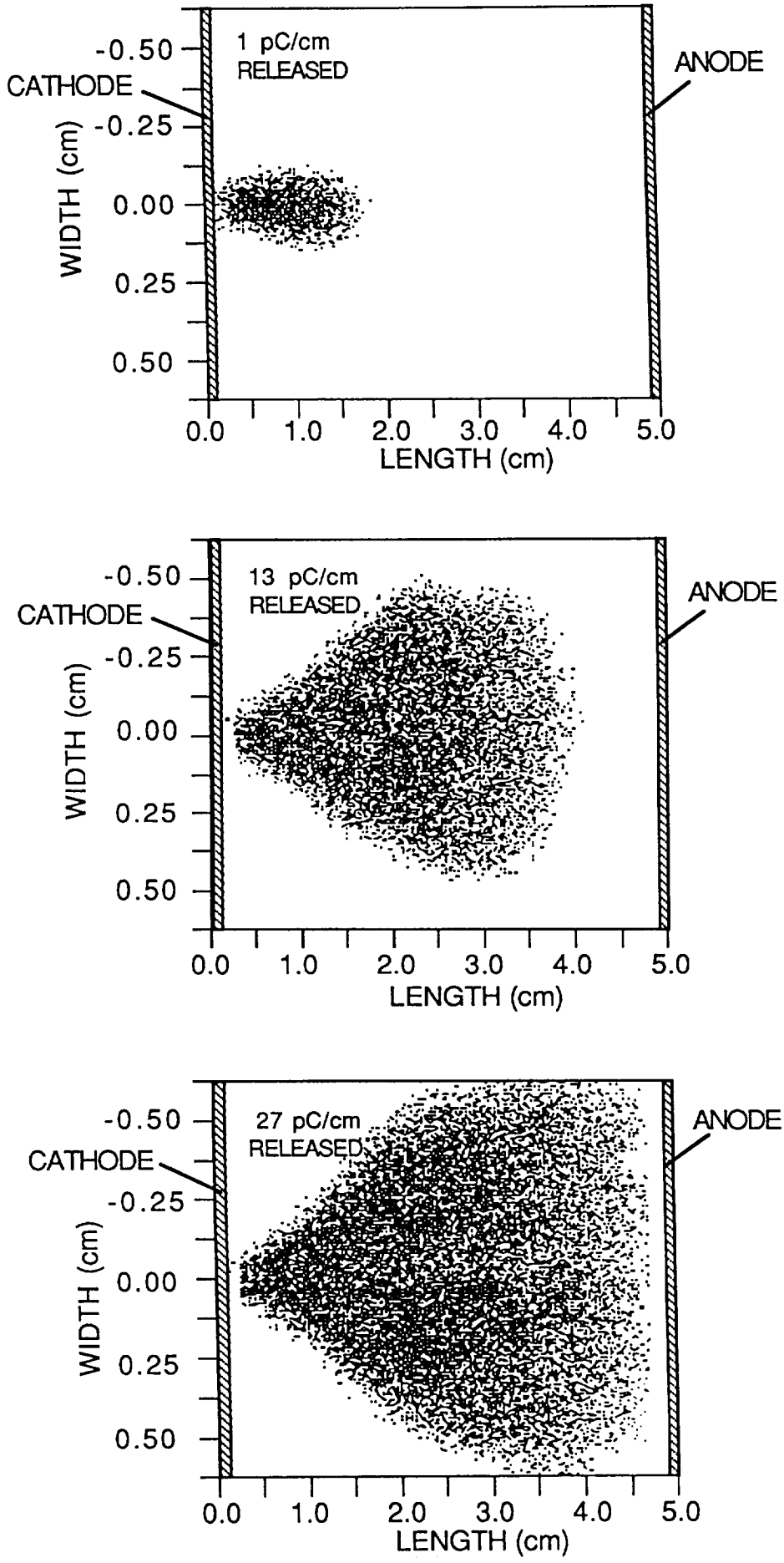
1 pC/cm
RELEASED
CATHODE
ANODE
-0.50
-0.25
0.00
0.25
0.50
WIDTH (cm)
0.0
1.0
2.0
3.0
4.0
5.0
LENGTH (cm)
13 pC/cm
RELEASED
CATHODE
ANODE
-0.50
-0.25
0.00
0.25
0.50
WIDTH (cm)
0.0
1.0
2.0
3.0
4.0
5.0
LENGTH (cm)
27 pC/cm
RELEASED
CATHODE
ANODE
-0.50
-0.25
0.00
0.25
0.50
WIDTH (cm)
0.0
1.0
2.0
3.0
4.0
5.0
LENGTH (cm)

Figure 6

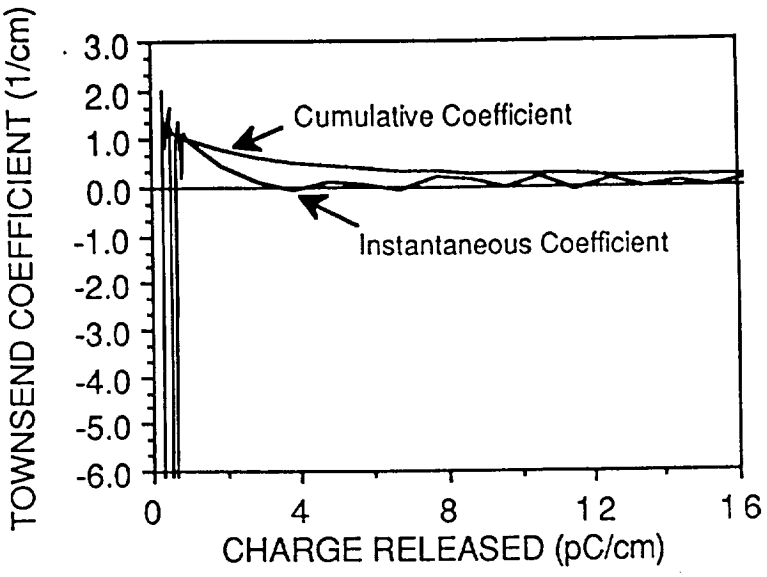

Figure 7

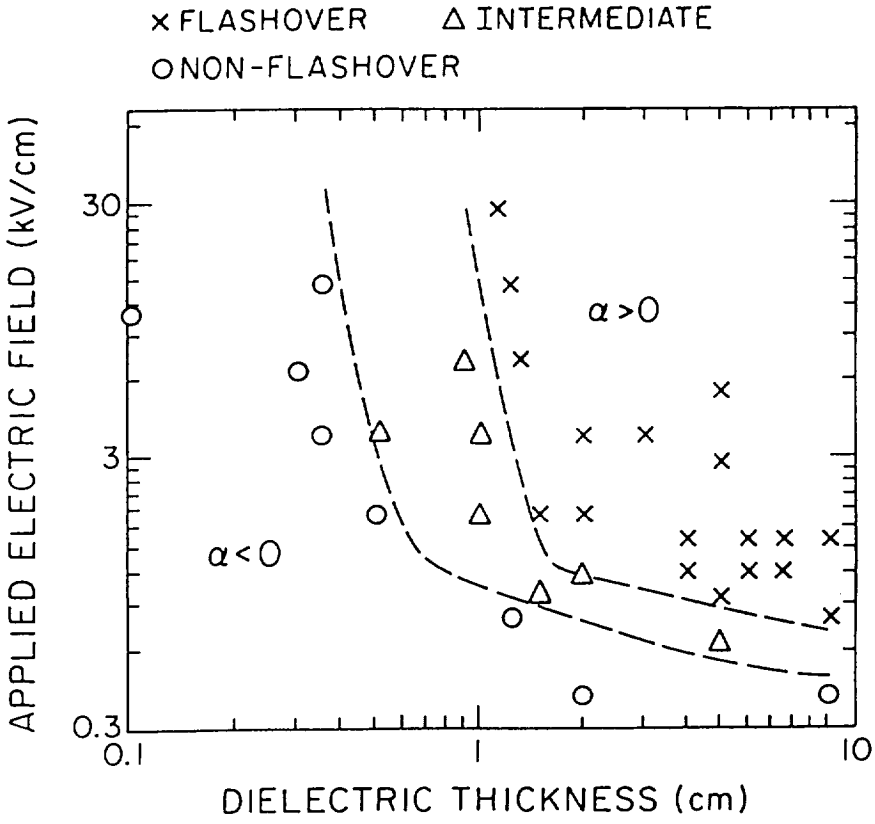

Figure 8

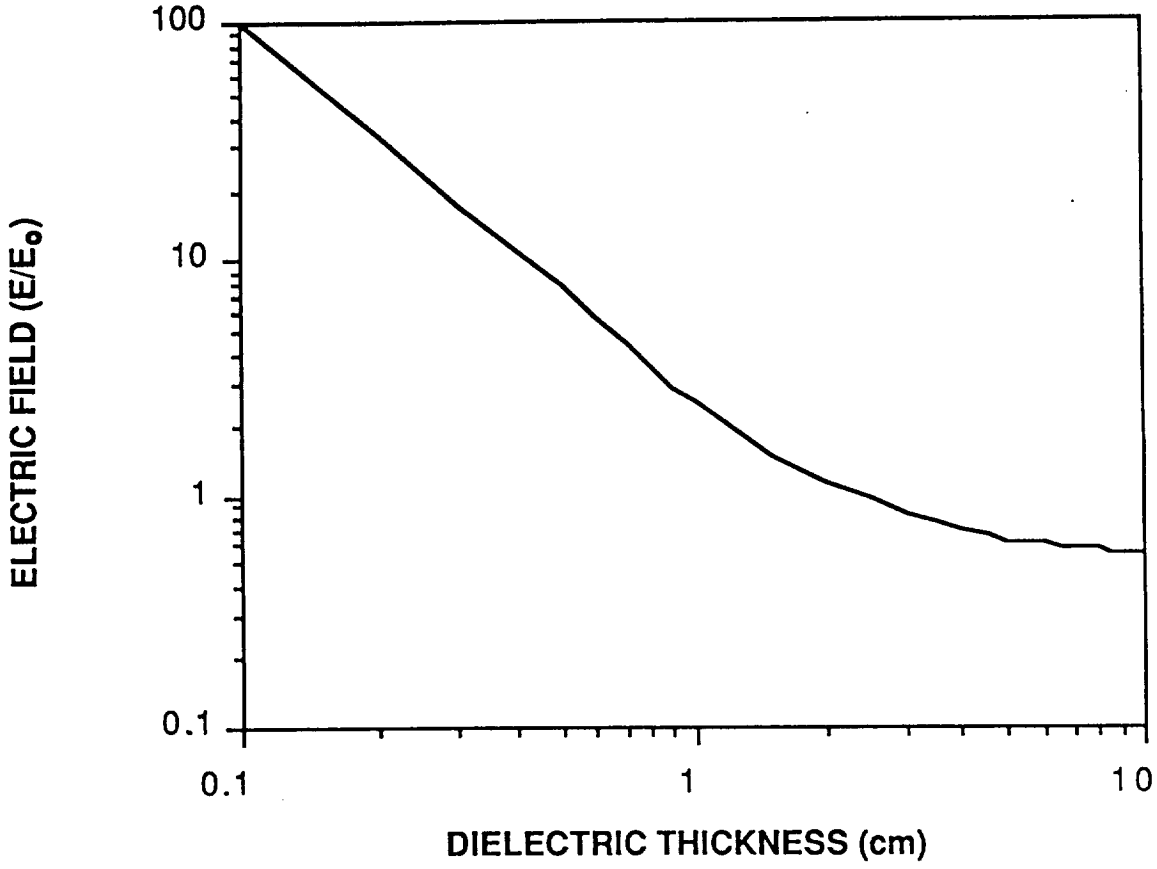
100
10
1
0.1
0.1
1
10
ELECTRIC FIELD (E/E$_o$)
DIELECTRIC THICKNESS (cm)

Figure 9

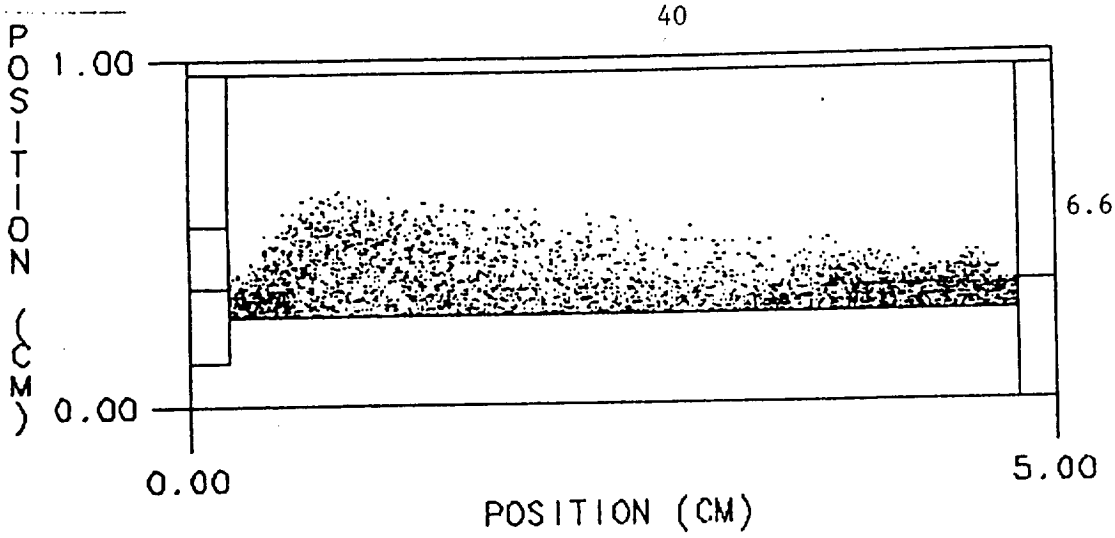

Vacuum

6.6 ns < "1-100" < 31 ns

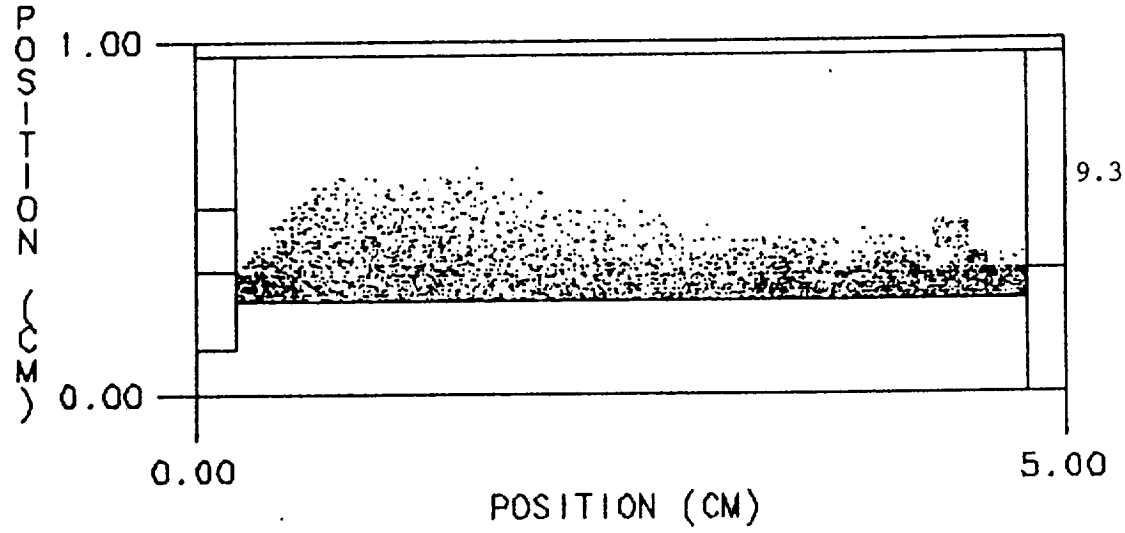

500 Torr He

9.3 ns < "1-100" < 33 ns

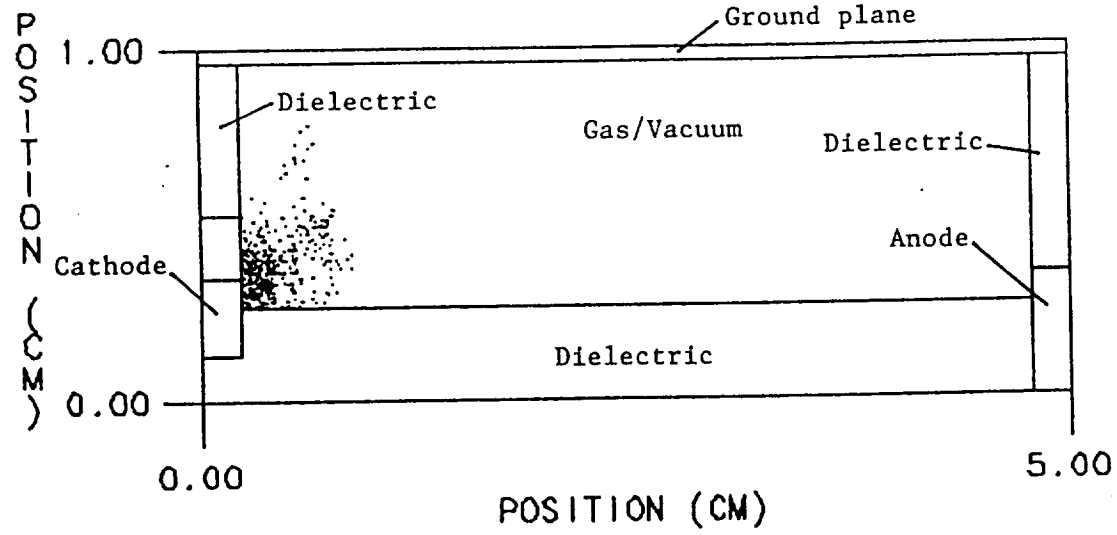

10 Torr F_2

250 ns << "1-100"
(no crossings
recorded)

Figure 10

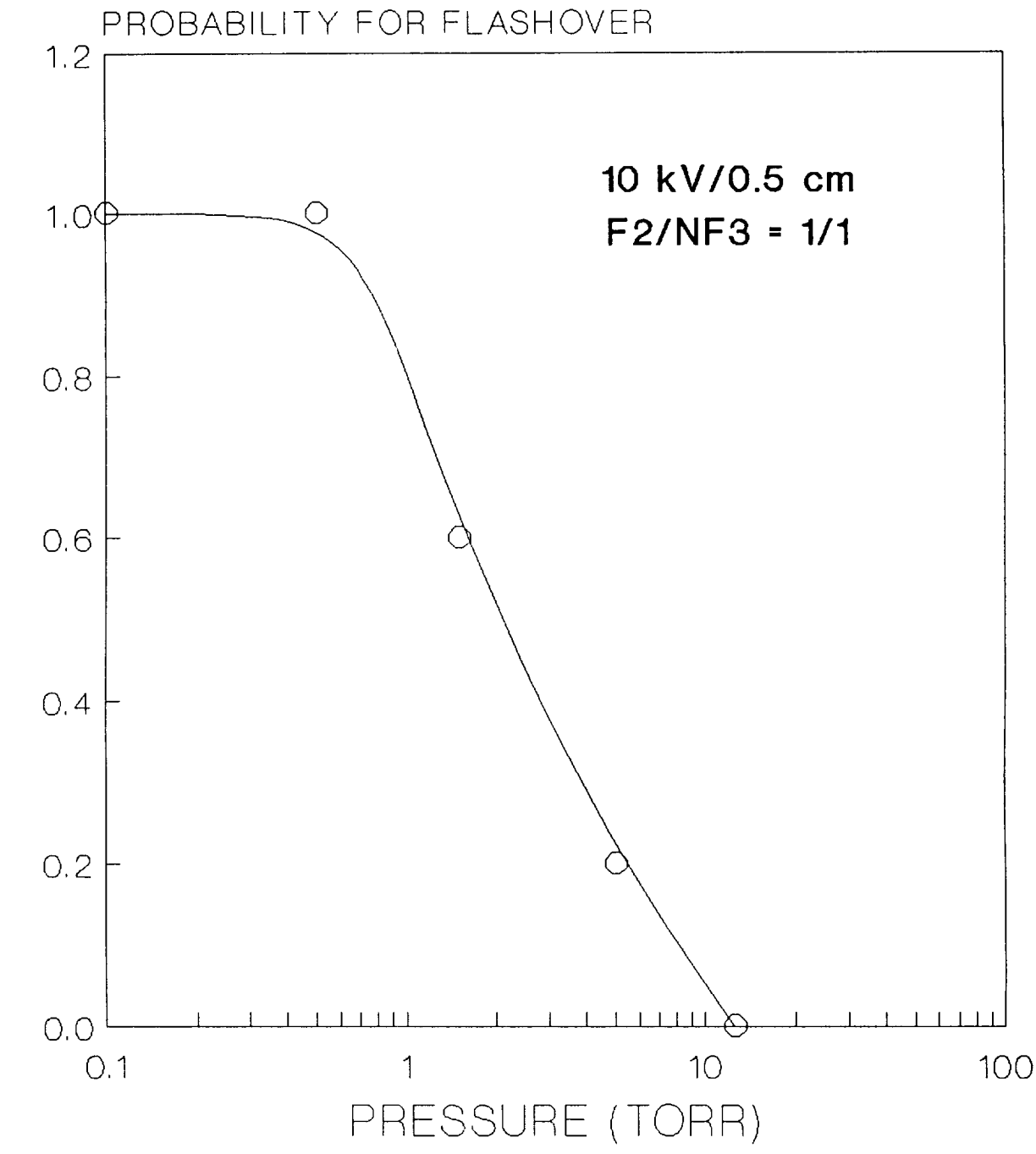

NASLEW7A

Figure 11

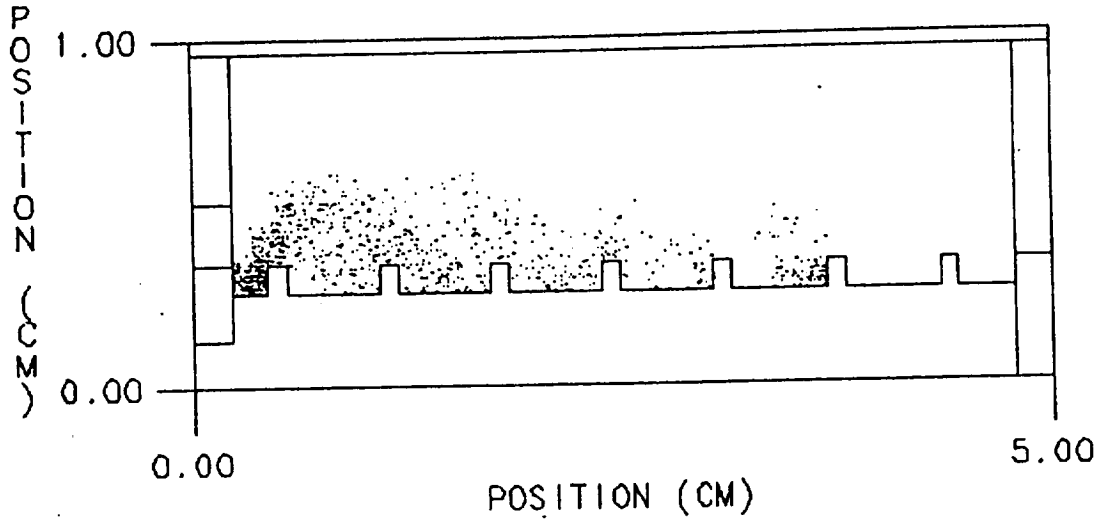

t = 30 ns

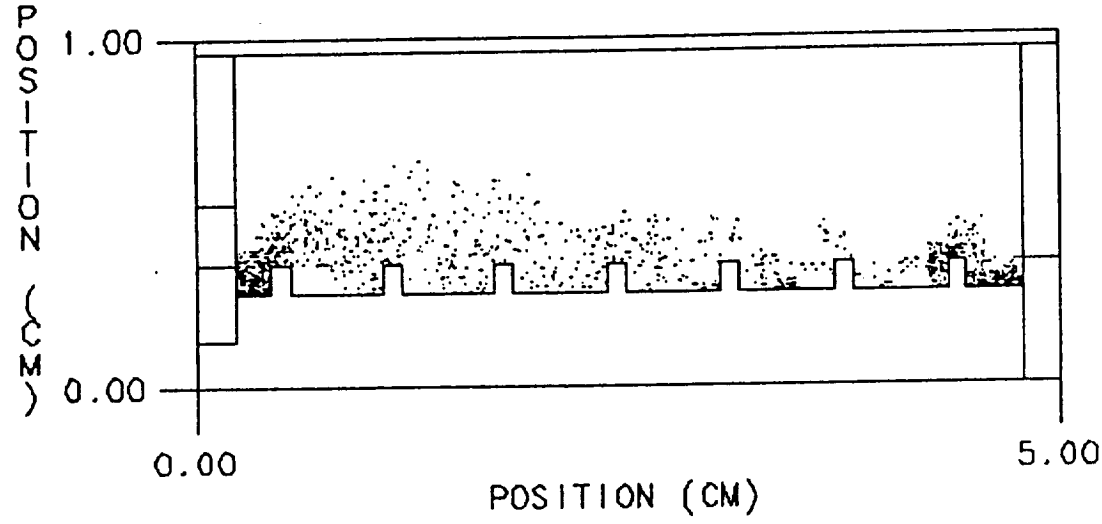

t = 50 ns

Figure 12

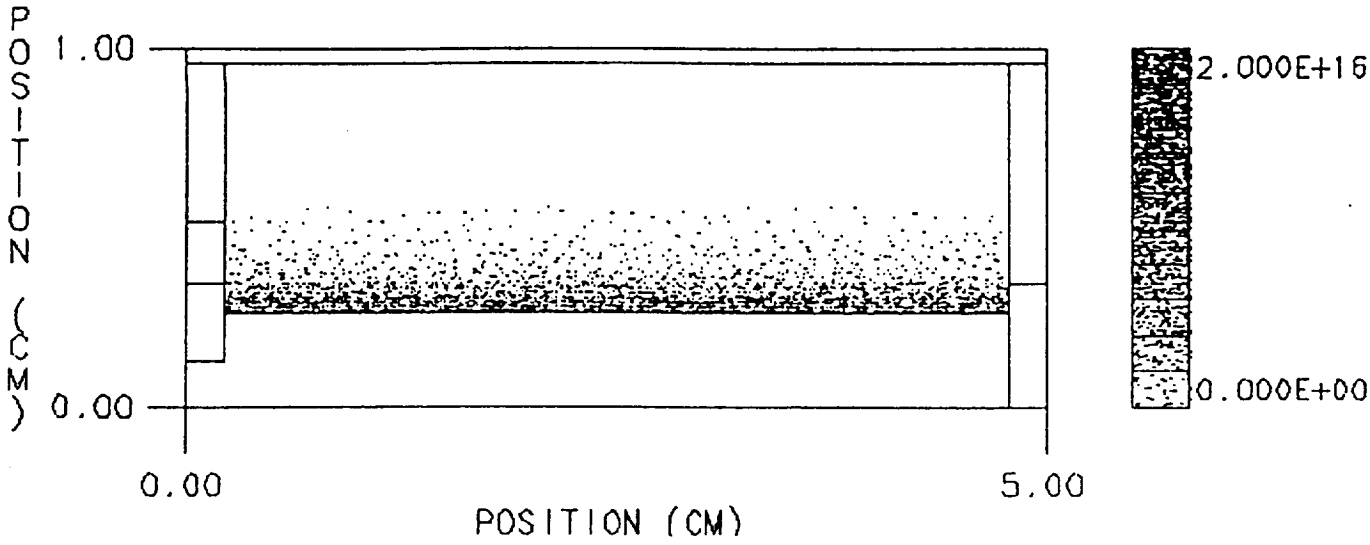

Figure 13

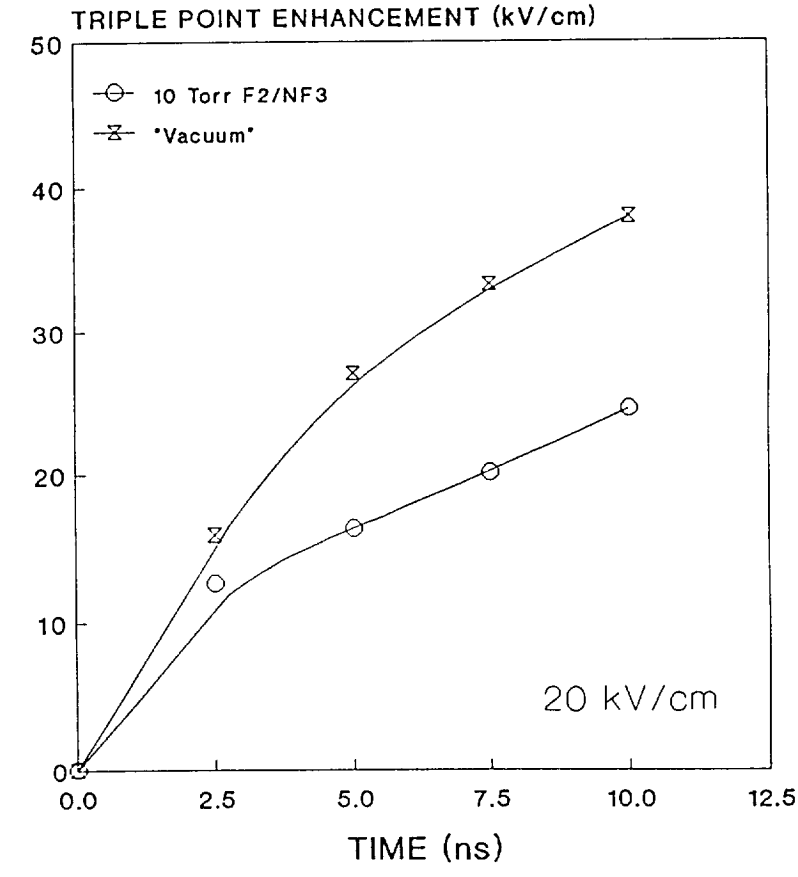

NALEW32

Figure 14

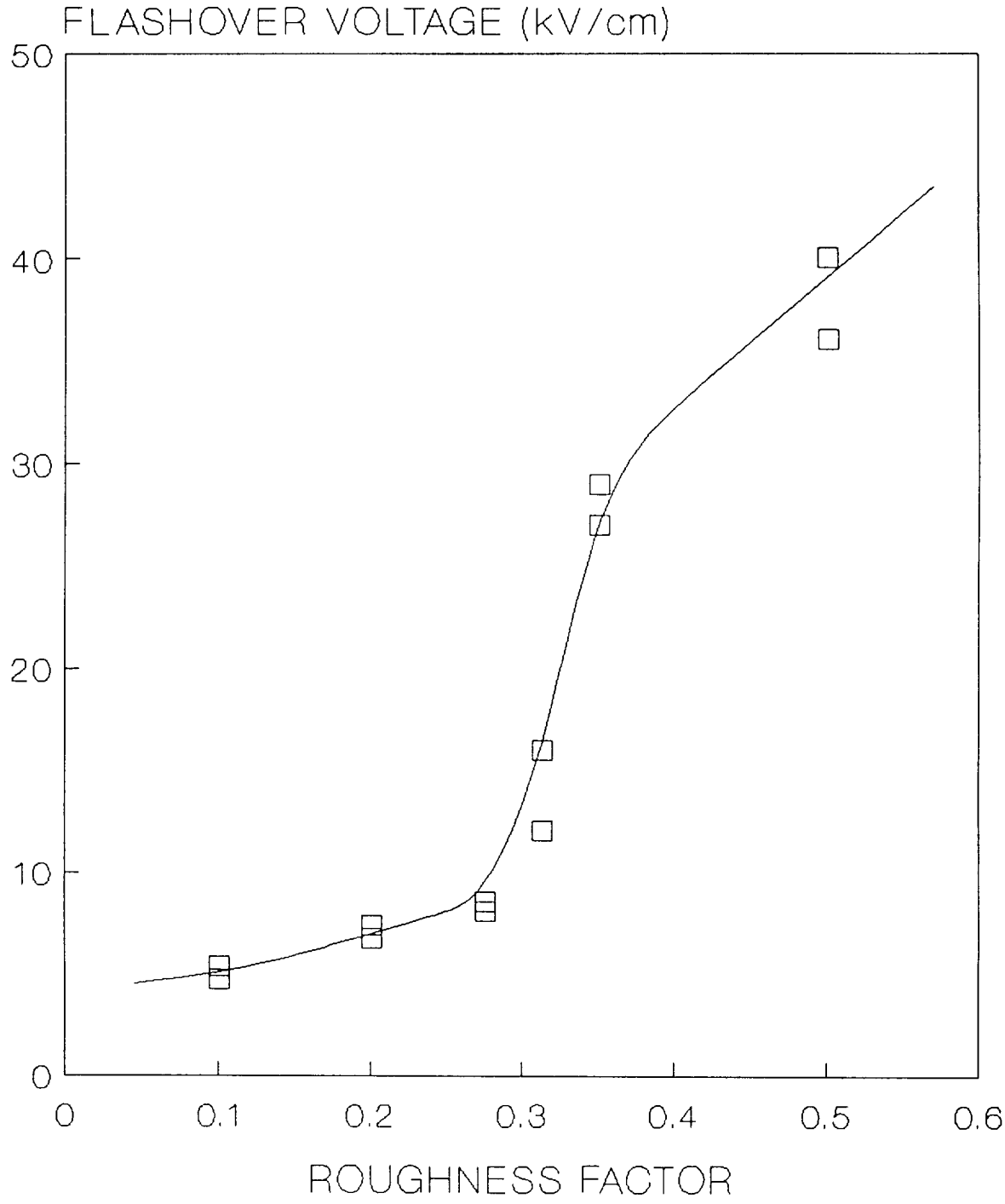

NALEW11

Figure 15

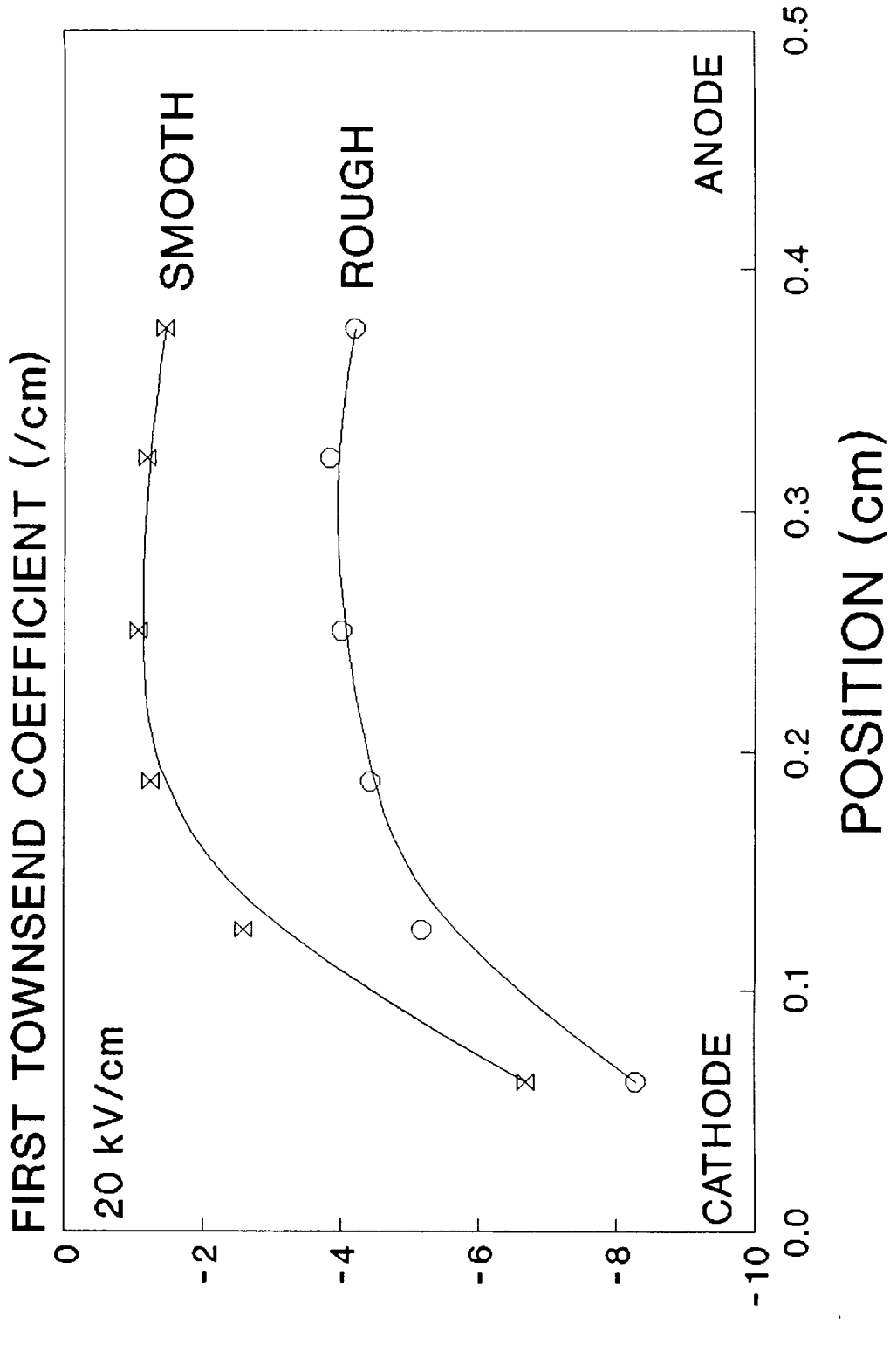
FIRST TOWNSEND COEFFICIENT (/cm)
20 kV/cm
SMOOTH
ROUGH
CATHODE
ANODE
POSITION (cm)
0
-2
-4
-6
-8
-10
0.0
0.1
0.2
0.3
0.4
0.5
NALEW30

Figure 16

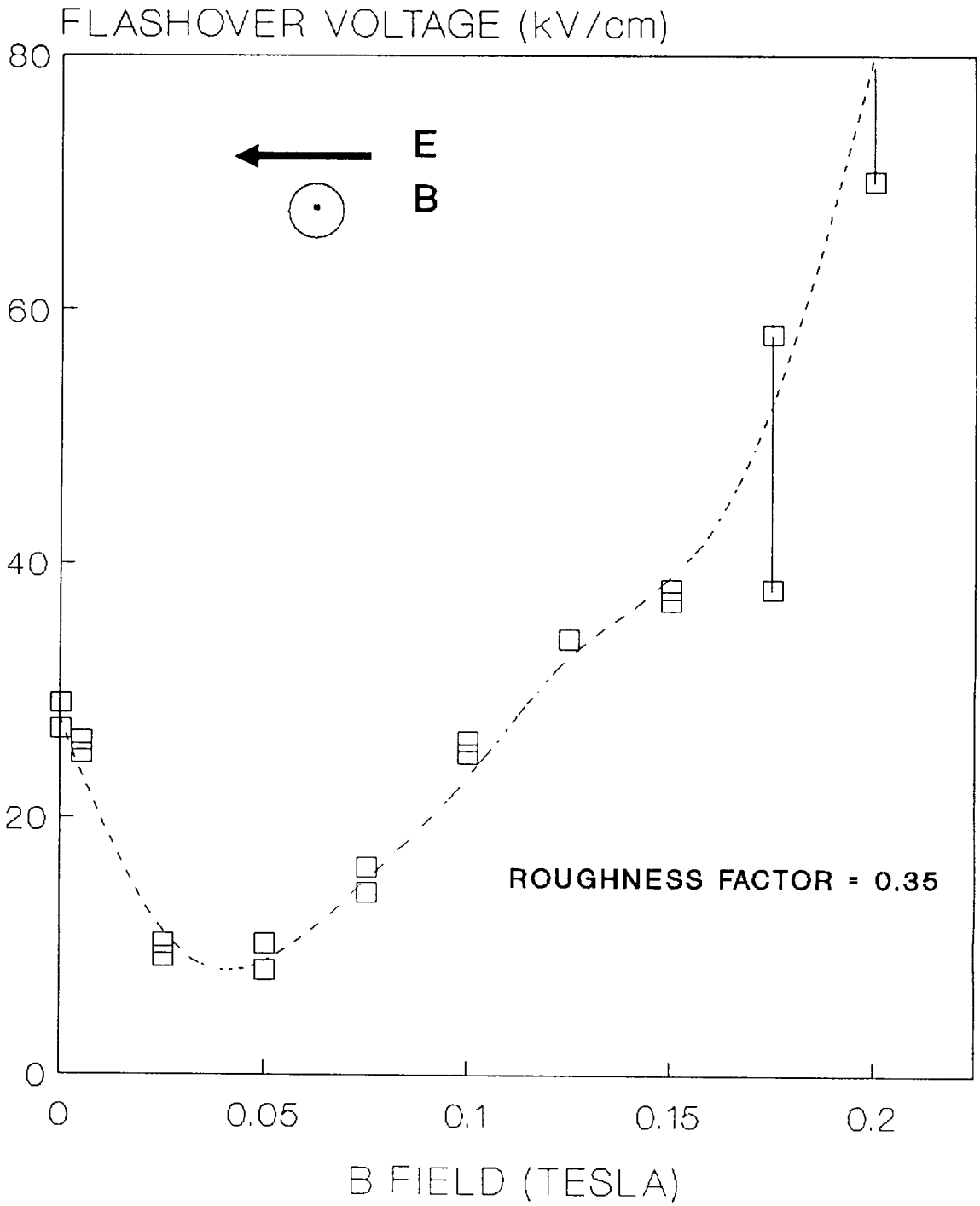

NALEW20A

Figure 17

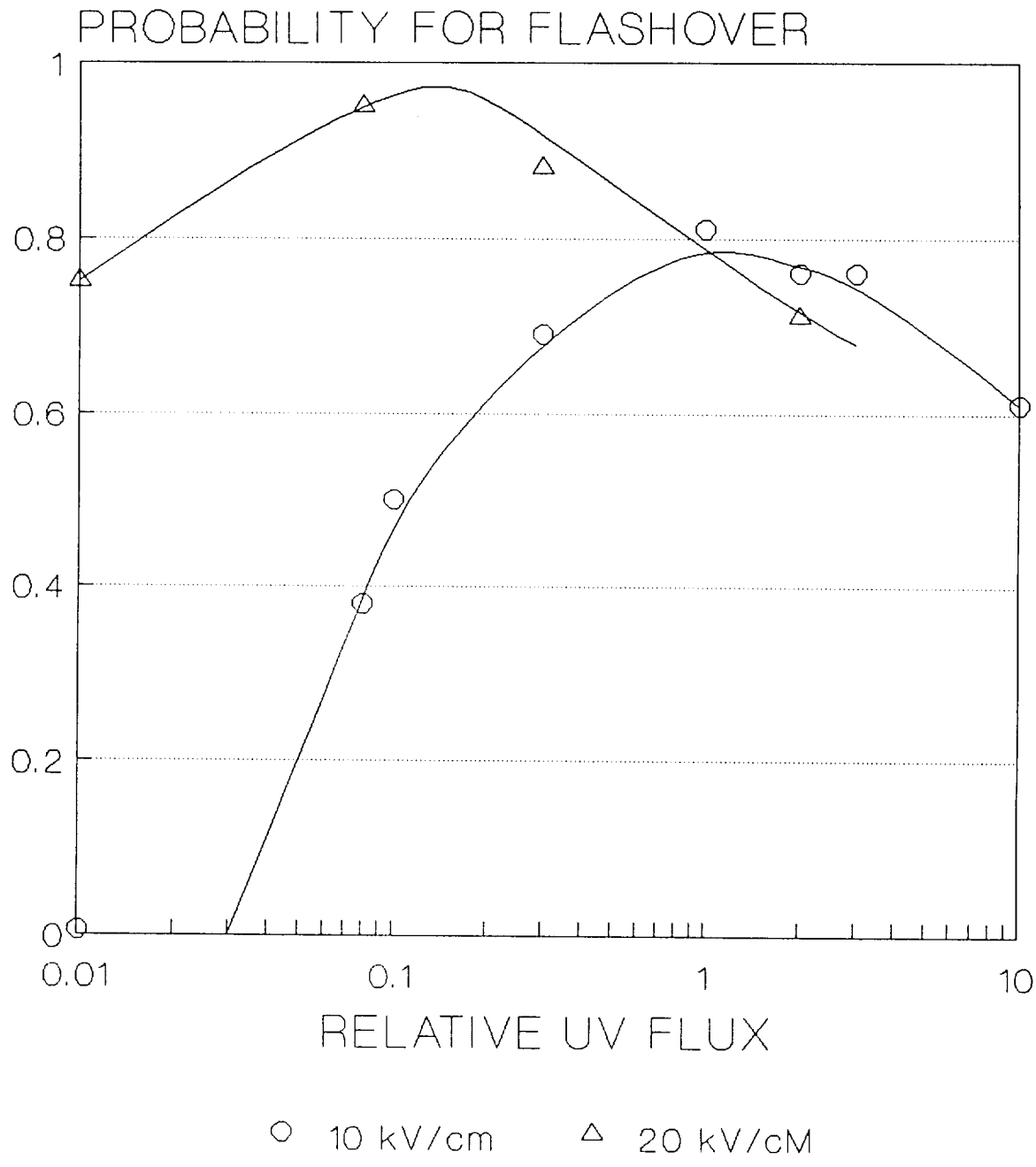

NASLEW9A

Figure 18